

BRIEF REPORTS

Brief Reports are accounts of completed research which, while meeting the usual Physical Review B standards of scientific quality, do not warrant regular articles. A Brief Report may be no longer than four printed pages and must be accompanied by an abstract. The same publication schedule as for regular articles is followed, and page proofs are sent to authors.

Influence of pressure on structural and magnetic phase transitions in $\text{La}_{0.835}\text{Sr}_{0.165}\text{MnO}_3$

K. Kamenev,* G. Balakrishnan, M. R. Lees, and D. McK. Paul
Department of Physics, University of Warwick, Coventry CV4 7AL, United Kingdom

Z. Arnold and O. Mikulina
Institute of Physics, Academy of Sciences of Czech Republic, Cukrovarnická 10, 162 00 Prague 6, Czech Republic
 (Received 21 January 1997)

Measurements of the thermal expansion of a single crystal of $\text{La}_{0.835}\text{Sr}_{0.165}\text{MnO}_3$ were performed under hydrostatic pressure of up to 9 kbar. The P - T phase diagram is established for the structural and magnetic phase transitions. Pressure is found to enhance the ferromagnetic coupling and to weaken the stability of the low-temperature orthorhombic phase by reducing the bending of the Mn-O-Mn bond. The decrease in the temperature T_S of the structural phase transition and the increase in the Curie temperature with increasing pressure leads to the two phase boundaries crossing at a pressure of about 3 kbar. The peculiar behavior of the T_S and T_C in the vicinity of the crossing point demonstrates a strong coupling between structural distortion and magnetic ordering in the $\text{La}_{0.835}\text{Sr}_{0.165}\text{MnO}_3$ compound. [S0163-1829(97)03629-1]

The series of $\text{La}_{1-x}\text{Sr}_x\text{MnO}_3$ perovskites exhibit a rich variety in the magnetic, structural, and electronic properties as the Sr content increases. The parent compound LaMnO_3 is an antiferromagnetic insulator below 140 K. The electronic configuration of the Mn atoms is $t_{2g}e_g$ (spin quantum number is $S=2$). The electrons of the t_{2g} bands are localized near the Mn ion sites, but the e_g electrons are hybridized with the oxygen $2p$ states creating chemical Mn-O-Mn bonds. Chemical substitution of La^{3+} by divalent Sr introduces Mn^{4+} ions into the lattice and holes into the e_g band. The ‘‘double-exchange’’ interaction between the Mn^{3+} and the Mn^{4+} ions causes a ferromagnetic metallic (FMM) ground state to appear for $x>0.15$.^{1,2} The Mott transition between the paramagnetic insulating (PMI) and conducting FM phases is accompanied by a thousandfold decrease in resistivity as a magnetic field is applied. This effect is called ‘‘colossal’’ magnetoresistance (CMR) and has a considerable potential for certain sensor applications. CMR has recently attracted considerable experimental and theoretical interest in the perovskite manganites.

The doping of Sr also results in a change in the structural ordering from the orthorhombic ($Pbnm$; $Z=4$) space group

to the rhombohedral ($R\bar{3}c$; $Z=2$) one. With increasing x , the room-temperature structure changes to $R\bar{3}c$ at x of about 0.17.¹ The x - T phase diagram shows that the magnetic and structural properties are extremely sensitive to the Sr doping in this region. The Curie temperature T_C of the paramagnetic to ferromagnetic phase transition increases from 238 K for $x=0.15$ to 283 K for $x=0.175$, whereas the temperature T_S of the $Pbnm$ - $R\bar{3}c$ structural transition decreases from 380 to 190 K.³

The fact that for $x\sim 0.17$ the temperatures T_S and T_C are close to each other has made it possible to induce the structural phase transition to an orthorhombic state by an applied magnetic field.⁴ In the present study we apply hydrostatic pressure to a single crystal of $\text{La}_{0.835}\text{Sr}_{0.165}\text{MnO}_3$ in order to investigate the influence of pressure on the stability of the magnetic and structural phases.

Single crystals of $\text{La}_{0.835}\text{Sr}_{0.165}\text{MnO}_3$ were grown from polycrystalline rods in an infra-red image furnace using the floating-zone method. The precursor materials were prepared by mixing appropriate quantities of La_2O_3 , SrCO_3 , and MnO_2 . The powder was ground and calcined three times at 1300 °C for 12 h and then pressed into rods which were

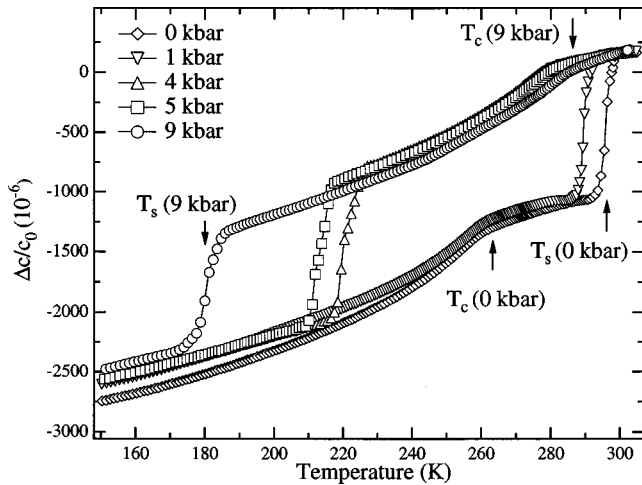


FIG. 1. The thermal expansion $\Delta c/c_0$ vs temperature T for heating runs at starting pressure of 0, 1, 4, 5, 9 kbar. The c_0 values are taken at $T=293$ K. The Curie temperature T_C and T_S are marked with arrows for the runs at 0 and 9 kbar.

sintered at 1400°C for 12 h. Laue x-ray photographs showed that the samples were high-quality single crystals.

The thermal expansion and compressibility were measured by microstrain gauges (Micro-Measurements Inc., SK-350) glued on bar-shaped samples. The strain gauges were calibrated using data for the thermal expansion and compressibility of silica, Cu, and Fe as references. The pressure measurements were performed in a CuBe pressure cell with a fixed hydrostatic pressure up to 9 kbar. A mixture of mineral oils was used as a pressure transmitting medium. Pressure and temperature were measured *in situ* using a calibrated manganin pressure sensor and a Thermocoax thermocouple, respectively.

The thermal expansion was measured along the threefold c axis of a $\text{La}_{0.835}\text{Sr}_{0.165}\text{MnO}_3$ single crystal. The set of the curves representing the temperature dependence of $\Delta c/c_0$ for heating runs at several pressures is shown in Fig. 1. It should be noted that because of differences in the thermal-expansion coefficients of the pressure transmitting medium and the pressure cell, the pressure inside the cell decreased as the temperature lowered. The actual values of pressure at T_C and T_S for cooling and heating runs are presented in Table I.

There are two anomalies on each of the curves corresponding to the magnetic phase transition from paramagnetic

TABLE I. The starting pressures at room temperature; the values of T_C and T_S for different pressure cycles measured during the cooling and heating runs; P_C and P_S are the actual values of pressure at T_C and T_S , respectively.

Starting pressure kbar	Cooling				Heating			
	T_C K	P_C kbar	T_S K	P_S kbar	T_C K	P_C kbar	T_S K	P_S kbar
0	262	0.0	292	0.0	263	0.0	296	0.0
1	263	0.7	286	1.0	263	0.0	289	1.1
4	279	4.0	212	2.9	278	4.0	220	3.0
5	280	4.9	203	3.8	281	5.0	213	3.8
9	287	8.9	170	7.0	286	8.9	180	7.2

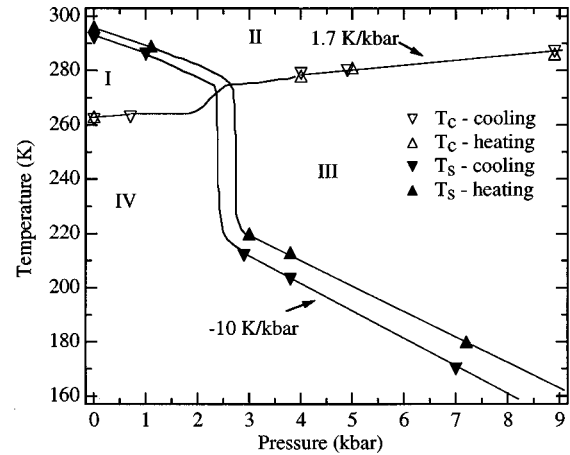


FIG. 2. Magnetic and structural P - T phase diagram of $\text{La}_{0.835}\text{Sr}_{0.165}\text{MnO}_3$; the phases are marked according to the types of magnetic and structural ordering: I-PMI+ $Pbnm$; II-PMI+ $R\bar{3}c$; III-FMM+ $R\bar{3}c$; IV-FMM+ $Pbnm$. The lines are guides for eyes.

to ferromagnetic phase (T_C) and to the structural phase transition from rhombohedral to orthorhombic phase (T_S), respectively. For ambient pressure, $T_C=263$ K and $T_S=296$ K, which is in a good agreement with the results of the direct observations of these transitions by means of neutron diffraction.⁵ The first-order transition to the orthorhombic phase is accompanied by a lattice shrinkage of about 0.12% along the threefold axis. The $\Delta c/c_0$ for the magnetic phase transition is small. The absolute value of this change in $\Delta c/c_0$ is rather difficult to estimate because the phase transition is second order and thus is spread to the higher temperature region ($T>300$ K).

As pressure increases, the magnitude of the $\Delta c/c_0$ changes remains the same but the positions of the anomalies shift in temperature as the Curie temperature T_C increases, while T_S rapidly decreases. The results of the pressure study are summarized in the P - T phase diagram presented in Fig.

2. The crossing point of the PM-FM and $R\bar{3}c$ - $Pbnm$ phase transition can be reached at 270 K by applying a pressure of about 3 kbar. As a result of the strong coupling of the magnetic and structural properties in this material, the pressure dependence of the Curie temperature and the temperature of structural phase transition are remarkably nonlinear in the vicinity of the crossing point. As pressure increases from 1 to 3 kbar, the temperature T_S decreases from 290 to 220 K whereas T_C increases from 263 to 278 K.

Above $P=3$ kbar the structural and magnetic phase transitions are well separated in temperature and the pressure dependences of T_S and T_C become linear. The slope of dT_C/dP can be estimated as 1.7 K/kbar, which is in a good agreement with the value reported in Ref. 6. The gradient for T_S on the P - T phase diagram is -10.0 K/kbar. The structural phase transition becomes extremely hysteretic at lower temperatures with the width of the hysteresis loop increasing from 4 to 10° as T_S decreases from 292 to 170 K (Table I and Fig. 2). The sharp decrease of T_S near the crossing point makes it difficult to study this part of the phase boundary in a pressure cell using oil as a transmitting medium. Such equipment only allows us to perform temperature variations

at constant pressure, due to the fact that oil becomes solid below its freezing temperature and cannot be compressed hydrostatically. More careful investigation of the critical temperatures in the vicinity of the crossing point should be made in a cell utilizing gaseous helium as a pressure-transmitting medium which would make it possible to vary pressure at constant temperature.

Figure 2 shows that there are four distinct regions to the P - T phase diagram due to the existence of the crossing point. Each of these phases is a combination of different types of magnetic and structural ordering: I-PMI+ $Pbnm$; II-PMI+ $R\bar{3}c$; III-FMM+ $R\bar{3}c$; IV-FMM+ $Pbnm$. Our recent neutron-diffraction measurements in the Institut Laue-Langevin (Grenoble, France) have confirmed that the high-pressure structural and magnetic phases have the same symmetry as those at ambient pressure,⁷ i.e., there are no additional or intermediate structural or magnetic phase transitions produced by the application of pressure. The $\text{La}_{1-x}\text{Sr}_x\text{MnO}_3$ series of compounds provides a unique opportunity to study on one compound the magnetic transformations in two different structural phases and *vice versa*, the same structural change in both a magnetically ordered FMM and a disordered PMI state.

Interestingly, for $\text{La}_{1-x}\text{Sr}_x\text{MnO}_3$ ($x \sim 0.165$) the crossing point can be reached not only by the application of external pressure but also by application of magnetic field^{4,8} and by an increase of Sr content.⁸⁻¹⁰ Comparing the x - T ,^{8,9} H - T ,⁴ and P - T (present study) phase diagrams reveals a common tendency in behavior, i.e., an increase of x , H , or P leads to *increase* of T_C and *decrease* of T_S . A qualitative explanation of this fact may be given in terms of the interplay between structural distortion and the kinetic energy of the e_g charge carriers.

There have been quite a few reports on the key role which the value of the tolerance factor t plays in determining the properties of the Mn system. The t factor provides a measure of the mismatch which occurs on doping of divalent ions (Sr, in the present case) and consequent bending of the Mn-O-Mn

bond.¹⁰⁻¹² The deviation of the Mn-O-Mn bond angle from 180° weakens the transfer interaction and, *vice versa*, the decrease in the transfer interaction tends to increase the bending of the Mn-O-Mn bond. In the perovskite-like structures the Mn-O-Mn angle in the orthorhombic phase is larger than in the rhombohedral one.¹⁰

The applied magnetic field directly influences the t_{2g} local spins tending to align them. This enhances the ferromagnetic coupling and leads to an *increase* of the Curie temperature T_C . Then, as follows from the Kondo calculations,^{13,14} the spin-polarized e_g electrons are scattered less by the electrons of the t_{2g} band. As a consequence, the conduction electrons become more itinerant as their transfer energy increases. This favors the rhombohedral structure and thus *reduces* the temperature T_S .

The application of pressure (either external or ‘‘chemical’’) decreases the bending of the Mn-O-Mn bond favoring the rhombohedral structural ordering and thus *decreasing* T_S . As regards the magnetic sublattice, such an increase of the Mn-O-Mn angle reduces the effective mass of the charge carriers increasing their transfer interaction. The enhanced ferromagnetic coupling leads to an *increase* in T_C .

In summary, we have performed the measurements of the thermal expansion on a single crystal of $\text{La}_{0.835}\text{Sr}_{0.165}\text{MnO}_3$ at different pressures, and have established the P - T phase diagram for this material. Applied pressure enhances the ferromagnetic coupling increasing the Curie temperature and weakens the stability of the orthorhombic phase decreasing T_S . The boundaries delineating the structural and magnetic phase transitions cross at about 270 K, under a pressure of about 3 kbar. The nonlinear shape of both structural and magnetic phase boundaries in the vicinity of the crossing point demonstrates a strong coupling between structural distortion and magnetic ordering.

This work was supported by EPSRC Grant No. GR/K95802.

* Author to whom correspondence should be addressed; electronic address: pbsch@csv.warwick.ac.uk; FAX: (44) 1203 692016.

¹A. Urushubara, Y. Moritomo, T. Arima, A. Asamitsu, G. Kido, and Y. Tokura, *Phys. Rev. B* **51**, 14 103 (1995).

²H. Kawano, R. Kajimoto, M. Kubota, and H. Yoshizawa, *Phys. Rev. B* **53**, 2202 (1996).

³Y. Tokura, A. Urushubara, Y. Moritomo, T. Arima, A. Asamitsu, G. Kido, and N. Furukawa, *J. Phys. Soc. Jpn.* **63**, 3931 (1994).

⁴A. Asamitsu, Y. Moritomo, Y. Tomioka, T. Arima, and Y. Tokura, *Nature (London)* **373**, 407 (1995).

⁵A. J. Campbell, G. Balakrishnan, M. R. Lees, D. McK. Paul, and G. J. McIntyre, *Phys. Rev. B* **55**, R8622 (1997).

⁶Y. Moritomo, A. Asamitsu, and Y. Tokura, *Phys. Rev. B* **51**, 16 491 (1996).

⁷K. Kamenev, G. Balakrishnan, M. R. Lees, D. McK. Paul, and

G. McIntyre (unpublished).

⁸Y. Tokura *et al.*, *J. Phys. Soc. Jpn.* **63**, 3931 (1994).

⁹H. Kawano, R. Kajimoto, M. Kubota, and H. Yoshizawa, *Phys. Rev. B* **53**, R14709 (1996).

¹⁰J. B. Goodenough and J. M. Longo, in *Magnetische und andere Eigenschaften von Oxiden und verwandten Verbindungen*, edited by K.-H. Hellwege and A. M. Hellwege, Landolt-Börnstein Tabellen Series, Vol. III/4a (Springer, Berlin, 1970), pp. 126–314.

¹¹J. Foncuberta, B. Martinez, A. Seffar, S. Piñol, J. L. García-Muñoz, and X. Obrados, *Phys. Rev. Lett.* **76**, 1122 (1996).

¹²R. Mahesh, R. Mahendiran, A. K. Raychaudhuri, and C. N. R. Rao, *J. Solid State Chem.* **120**, 204 (1995).

¹³N. Furukawa, *J. Phys. Soc. Jpn.* **63**, 3214 (1994).

¹⁴K. Kubo and N. Ohata, *J. Phys. Soc. Jpn.* **33**, 21 (1972).